applied sciences

MDPI

Article

Strength Criterion of Asphalt Mixtures in Three-Dimensional Stress States under Freeze-Thaw Conditions

Tuo Huang, Shuai Qi, Ming Yang, Songtao Lv *, Hongfu Liu and Jianlong Zheng

School of Traffic and Transportation Engineering, Changsha University of Science & Technology, Changsha 410114, China; ht@csust.edu.cn (T.H.); 17101030071@stu.csust.edu.cn (S.Q.); myang892018@126.com (M.Y.); lhf0625@csust.edu.cn (H.L.); zjl@csust.edu.cn (J.Z.)

* Correspondence: lst@csust.edu.cn; Tel.: +86-139-7519-7481

Received: 13 July 2018; Accepted: 1 August 2018; Published: 4 August 2018

Featured Application: This work provides the testing and theoretical reference for material and structure design of asphalt pavement in three-dimensional stress states under freeze-thaw conditions.

Abstract: In order to study the influence of freeze-thaw cycles on the multi-axial strength of AC (Asphalt Concrete)-13 and SMA (Stone Mastic Asphalt)-13 asphalt mixtures which are widely used in China, triaxial tests were carried out in the laboratory. Two nonlinear failure criterions under three-dimensional stress states in octahedral space were established. A linear model for engineering design and its simplified testing method were then presented. The three-dimensional failure criteria of asphalt mixtures after 0, 1, 3, 5, 10, 15, 20 freeze-thaw cycles were also proposed. The results indicated that the multi-axial strength decayed significantly after 20 freeze-thaw cycles. It is noteworthy that the strength degrades rapidly during the first 5 freeze-thaw cycles. Compared with AC-13 asphalt mixture, the SMA-13 asphalt mixture exhibits better performance on the resistance to freeze-thaw damage, and it is recommended as the upper surface layer material of pavement structure.

Keywords: asphalt mixtures; three-dimensional stress states; freeze-thaw cycles; triaxial strength; failure criterion

1. Introduction

Asphalt pavement is influenced by freeze-thaw cycles in the middle and lower reaches of the Yangtze River and some seasonally frozen areas of China in winter. Many studies have shown that freeze-thaw cycles significantly affect the performance of asphalt mixtures [1–3]. The freeze-thaw process would lead to the loss of adhesion between binder and aggregates, which can also change the properties of aggregate, such as strength, compressibility, porosity, and permeability [2], as well as reduce the strength and stiffness of asphalt mixtures. Therefore, it can cause various forms of premature pavement distress [3]. Some asphalt pavements were discovered to have grave freeze injury during construction right away or after the construction process is completed [4,5]. Hence, effective analysis of the freeze-thaw cycles on the performance of asphalt mixtures is necessary [6–8].

General studies are mainly focused on the influence of freeze-thaw cycles and the macro performance of asphalt mixtures under simple stress states including resistance, stiffness, stability, fatigue life, low-temperature properties, etc. [9–15]. They have made contributions to improve the accuracy of asphalt pavement design parameters. And a number of studies on the damage evolution of asphalt mixtures during freeze-thaw cycles from the basis of micro-level were reported in Ref. [16,17].

Furthermore, a lot of models were established to characterize the mechanical performance of asphalt mixtures after multiple freeze-thaw cycles under simple stress states [18,19].

However, the asphalt mixtures are not only affected by the freeze-thaw cycles, but also by the complex stress states in the site [20,21]. Therefore, the uniaxial tensile test, uniaxial compression test, bending test, and indirect test under one-dimensional or two-dimensional stress states cannot reflect the failure modes of asphalt mixtures in three-dimensional stress conditions in the asphalt pavement structures [22–24]. Generally speaking, the tensile properties of asphalt materials should be emphasized at relatively low temperature. While the conventional triaxial test is available only for the triaxial compressive stress state with confining pressure if the first principal stress σ_1 equal to the second principal stress σ_2, the triaxial tensile tests cannot be carried out [25–27]. As it is difficult to study the multi-axial strength properties of asphalt mixtures [28,29], the three-dimensional failure criterion of asphalt mixture after freeze-thaw cycles has not been developed.

The objective in this paper is to study the effects of the complex stress states and freeze-thaw in asphalt pavement in the laboratory, as well as to perform triaxial tests (especially triaxial tensile testing) for AC (Asphalt Concrete)-13 and SMA (Stone Mastic Asphalt)-13 asphalt mixtures after freeze-thaw cycles with the self-developed triaxial test method. In addition, the nonlinear and linear failure criterions under three-dimensional stress states are established to evaluate the impact of stress and freeze-thaw cycles on the performance of these asphalt mixtures. From the strength point of view, the SMA-13 asphalt mixture exhibits better freeze-thaw resistance under complex stress condition compared with the AC-13 asphalt mixture. Therefore, it is recommended as the upper surface layer material of pavement structure.

2. Laboratory Experimental Program

2.1. Materials

The continuous-graded AC(Asphalt Concrete)-13 and gap-graded SMA(Stone Mastic Asphalt)-13 asphalt mixtures, which are very commonly used for the surface layer on the highway and recommended by Technical Specifications for Construction of Highway Asphalt Pavements (JTG F40-2004) in China, were prepared for the experiment with its gradations listed in Figure 1. The basalt was used as aggregates and the SBS (Styrene Butadiene Styrene) modified bitumen (Zhonghai Asphalt (Taizhou) Co.,Ltd., Taizhou, China) was used as a binder for the preparation of specimens. The basic properties of SBS modified bitumen are as shown in Table 1 and the properties of lignin fiber for the SMA-13 asphalt mixture are shown in Table 2.

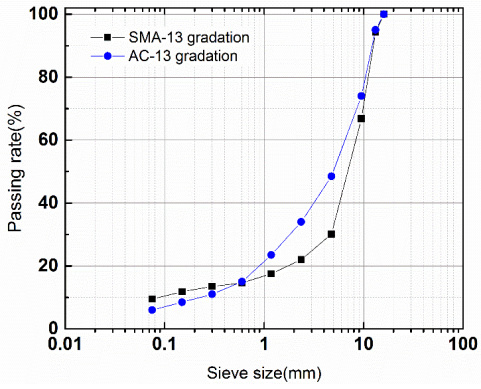

Figure 1. Chart of AC(Asphalt Concrete)-13 and SMA (Stone Mastic Asphalt)-13 gradations.

Table 1. Properties of SBS (Styrene Butadiene Styrene) modified bitumen.

Test	SBS Modified Bitumen	Technical Requirements
penetration (25 °C) (0.1 mm)	55.9	30~60
penetration index	0.53	>0
ductility (5 °C /cm, 5 cm/min)	34.2	≥20
softening point (°C)	79.4	≥60
viscosity (135 °C, Pa·s)	2.30	≤3

Table 2. Properties of fiber.

Test	Lignin Fiber	Technical Requirements
fiber length (mm)	3.5~4.8	≤6
ash content (%)	15.9	18 ± 5
pH value	7.12	7.5 ± 1.0
oil absorption (%)	841	≥500
moisture content (%)	1.29	≤5.0
density (g/cm^3)	0.938	/

The solid cylindrical specimens were made by the gyratory compactor (TIPTOP China Limited, Shanghai, China) with 100 mm diameter and 102 mm height. The performances of mixtures were extensively tested earlier by Huang [27,28]. The optimum asphalt-aggregates weight ratio of the AC-13 specimens was 5.2% with the air void content of 4.5%. The optimum asphalt-aggregates weight ratio of the SMA-13 specimens was 6.1% with the air void content 3.6%, and the content of the lignin fiber was 0.3%. Moreover, the two ends of the original specimen were polished by the diamond blade (Zhejiang Chenxin Machinery Equipment Co., Ltd, Shaoxing, China) up to the height of 100 mm. The hollow cylinder specimens with a dimension of 10 mm × 50 mm × 100 mm (inner radius × outer radius × height) were prepared for the triaxial tests by coring the solid cylinder specimens.

2.2. Testing Conditions and Procedures

2.2.1. Freeze-Thaw Cycles

The freeze-thaw experiments were carried out by repeating the freeze-thaw cycles according to the specification of the Standard Test Methods of Bitumen and Bituminous mixtures for Highway Engineering (JTG E20-2011) in China. Firstly, the specimens were immerged into the tap water in the water tank which was placed in the vacuum drying oven and kept the vacuum for 15 min under the condition of 97.3~98.7 kPa. Then, the valve was opened, the atmospheric pressure restored, and the specimens were placed in the water for 0.5 h. After that, we took out the specimens and put them into a plastic bag, added about 10 mL water and tightened the plastic bag. The specimens were put into the thermostats at the condition of −18 °C for 16 h. Finally, we took out the specimens and immediately put them in the water thermostat tank at 60 °C for 24 h. One freeze-thaw cycle was completed by following the above steps. The triaxial tests were conducted at the end of 0, 1, 3, 5, 10, 15, and 20 cycles.

2.2.2. Triaxial Test

The triaxial test method is used to characterize the mechanical properties of asphalt mixtures under complex stress states, especially in the triaxial tensile stress state, as shown in Figure 2. In this test, a hollow cylinder specimen was placed in the test equipment while the inner and outer surfaces of the specimen were loaded by two independent flexible airbags. Hence, adjustable radial compressive stress and circumferential tensile stress can be generated. Meanwhile, the axial tensile or compressive stresses were produced by a material testing system MTS (Mechanical Testing & Simulation systems company, Minneapolis, USA). Therefore, the three-dimensional unequal stress states can be generated to simulate the complex stress states of asphalt pavement materials in the pavement structures.

According to elastic mechanics, the principal stresses, including axial stress, σ_z, radial stress, σ_ρ, and circumferential stress, σ_φ, can be sorted numerically in terms of the principal stresses σ_1, σ_2, and σ_3, respectively [29].

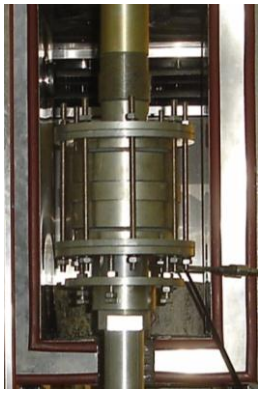

Figure 2. Diagram of triaxial test.

In order to simulate the weather of the middle and lower reaches of the Yangtze River and some seasonally frozen areas of China in winter, as shown in Figure 3, 5 °C was selected as the testing temperature. Before the test, the specimens were kept in the temperature control chamber for more than 6 h. The axial loading rate was 2 mm/min, which is the same as the loading rate of the uniaxial compressive test in the current specification.

Figure 3. Average temperature map of China in January 2018.

Before the triaxial compressive test, some measures have been taken to reduce the friction at the end of the specimen. For example, lubricant oil was smeared on the upper and lower surfaces of the specimen. During the triaxial tensile test, it is necessary to ensure that the specimen is broken without degumming [29]. The triaxial test procedures are as follow:

(1) Tensile meridian and compressive meridian: The tensile meridian/compressive meridian can be obtained by the triaxial tensile/compressive test. Three-direction isobaric stress condition ($\sigma_1 = \sigma_2 = \sigma_3$) of specimens were set at certain stress levels by applying the inner, outer airbags and loading shaft of MTS, and thereafter, the axial tensile/compressive stress σ_1/σ_3 was applied until the failure of the specimen. A series of tensile tests were carried out under different three-direction isobaric stress conditions to obtain the tensile meridian. Likewise, the compressive meridian can be obtained. On the tensile meridian and compressive meridian, the lode angle was equal to 0°and 60°, respectively. The stress path of the tensile meridian and compressive meridians are shown in Figure 4.

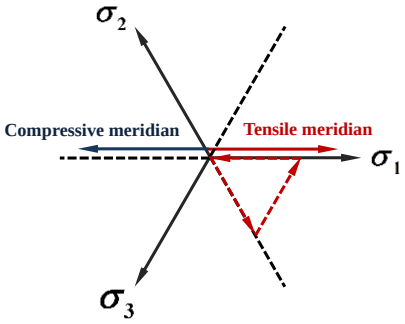

Figure 4. Stress path of tensile and compressive meridians.

(2) Strength envelope curve: The strength envelope curve can be obtained by plane tensile and compressive/axial tensile tests. At first, the transverse stresses, σ_2 and σ_3, were increased up to the pre-determined values proportionally by applying pressure with the inner airbag. Then, the axial tensile stress, σ_1, was applied by an MTS material testing machine until specimen failure. On the strength envelope curve, the average stresses were basically the same and the lode angles ranged from 0°~60° gradually. The stress path is shown in Figure 5 [28,29].

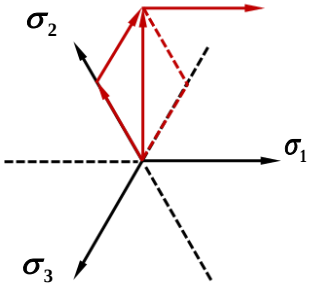

Figure 5. Stress path of strength envelope curve.

3. Failure Criterions

3.1. Nonlinear Failure Criterion

The average value of three effective test results of triaxial compressive/tensile tests, the plane tensile, and compressive/axial tensile tests are presented in Table 3. Based on the test results, the octahedral normal stress, σ_{oct}, octahedral shear stress, τ_{oct}, and lode angle, θ can be obtained by the following formulas [29]:

$$\sigma_{oct} = \sigma_m = (\sigma_1 + \sigma_2 + \sigma_3)/3 \tag{1}$$

$$\tau_{oct} = \sqrt{(\sigma_1 - \sigma_2)^2 + (\sigma_2 - \sigma_3)^2 + (\sigma_3 - \sigma_1)^2}/3 \tag{2}$$

$$\theta = \arccos\frac{2\sigma_1 - \sigma_2 - \sigma_3}{3\sqrt{2}\tau_{oct}} \tag{3}$$

Table 3. Results of triaxial tests for asphalt mixtures.

Test	Mixture Type	σ_1 (MPa)	σ_2 (MPa)	σ_3 (MPa)	$\frac{\sigma_{oct}}{f_c}$	$\frac{\tau_{oct}}{f_c}$	$\theta°$
triaxial compressive	AC-13	–	0.000	−8.477	−0.333	0.471	60
		−0.200	−0.200	−9.372	−0.384	0.510	60
		−0.400	−0.400	9.984	−0.424	0.533	60
		−0.600	−0.600	−10.750	−0.470	0.564	60
		−0.800	−0.800	−11.806	−0.527	0.612	60
	SMA-13	0.000	0.000	−9.240	−0.333	0.471	60
		−0.200	−0.200	−10.506	−0.393	0.526	60
		−0.400	−0.400	−10.983	−0.425	0.540	60
		−0.600	−0.600	−11.617	−0.462	0.562	60
		−0.800	−0.800	−12.969	−0.526	0.621	60
triaxial tensile	AC-13	1.110	0.000	0.000	0.044	0.062	0
		1.017	−0.500	−0.500	0.001	0.084	0
		0.913	−1.000	−1.000	−0.043	0.106	0
		0.700	−1.500	−1.500	−0.090	0.122	0
		0.588	−2.000	−2.000	−0.134	0.144	0
	SMA-13	1.258	0.000	0.000	0.045	0.064	0
		1.176	−0.500	−0.500	0.006	0.086	0
		1.059	−1.000	−1.000	−0.034	0.105	0
		0.864	−1.500	−1.500	−0.077	0.121	0
		0.748	−2.000	−2.000	−0.117	0.140	0
plane tensile and compressive/ axial tensile	AC-13	1.110	0.000	0.000	0.044	0.062	0
		1.091	0.125	−0.115	0.043	0.061	10.8
		1.042	0.313	−0.289	0.042	0.064	26.8
		0.991	0.442	−0.408	0.040	0.068	37.8
		0.987	0.505	−0.467	0.040	0.071	41.0
		0.955	0.594	−0.548	0.039	0.076	46.7
		0.896	0.780	−0.720	0.038	0.087	56.3
		0.834	0.834	−0.770	0.035	0.089	60
	SMA-13	1.258	0.000	0.000	0.045	0.064	0.0
		1.204	0.125	−0.115	0.044	0.062	9.8
		1.179	0.313	−0.289	0.043	0.065	24.1
		1.128	0.442	−0.408	0.042	0.068	33.5
		1.112	0.505	−0.467	0.041	0.070	37.6
		1.083	0.594	−0.548	0.041	0.074	43.0
		0.945	0.783	−0.720	0.036	0.081	54.9
		0.880	0.880	−0.810	0.034	0.086	60.0

For triaxial compressive tests, both AC-13 and SMA-13 specimens are mainly represented as shear failure shown in Figure 6. For the triaxial tensile test, the plane tensile, and compressive/axial tensile test, the specimen failures are shown in Figure 7.

Figure 6. Shear failure.

Figure 7. Tensile failure.

Based on the triaxial test results, the SMA-13 asphalt mixture has a higher strength in three-dimensional stress states (especially in triaxial tensile stress states) compared with AC-13 asphalt mixture. The three-dimensional nonlinear failure criterions of AC-13 and SMA-13 asphalt mixtures were established as follows:

Tensile meridian:

$$\frac{\tau_{oct}^{t}}{f_c} = a + b\frac{\sigma_{oct}}{f_c} + c\left(\frac{\sigma_{oct}}{f_c}\right)^2,\ R_{AC}^2 = 0.98; R_{SMA}^2 = 0.98 \tag{4}$$

Compressive meridian:

$$\frac{\tau_{oct}^{c}}{f_c} = d + e\frac{\sigma_{oct}}{f_c} + f\left(\frac{\sigma_{oct}}{f_c}\right)^2,\ R_{AC}^2 = 0.99; R_{SMA}^2 = 0.98 \tag{5}$$

Strength envelope curve:

$$\tau_{oct}(\theta) = \tau_{oct}^{t} - \left(\tau_{oct}^{t} - \tau_{oct}^{c}\right)\sin^n 1.5\theta,\ R_{AC}^2 = 0.96; R_{SMA}^2 = 0.97 \tag{6}$$

where f_c is the uniaxial compressive strength, a, b, c, d, e, f, and n are model parameters as shown in Table 4. The results of the experiments/prediction are presented in Figures 8 and 9, respectively.

Table 4. Parameters of the nonlinear failure criterions.

Mixture Type	*a*	*b*	*c*	*d*	*e*	*f*	*n*
AC-13	0.072	−0.55	−0.41	0.145	−1.138	−0.541	5
SMA-13	0.084	−0.664	−0.426	0.139	−1.095	−0.632	7

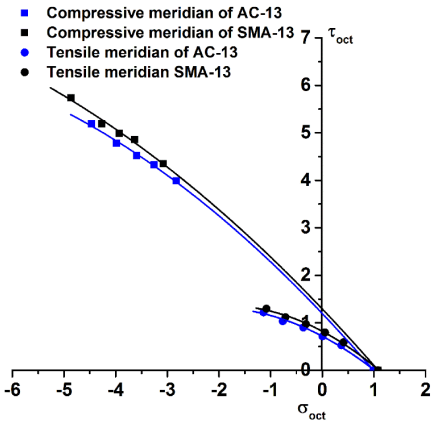

Figure 8. Nonlinear tensile and compressive meridians.

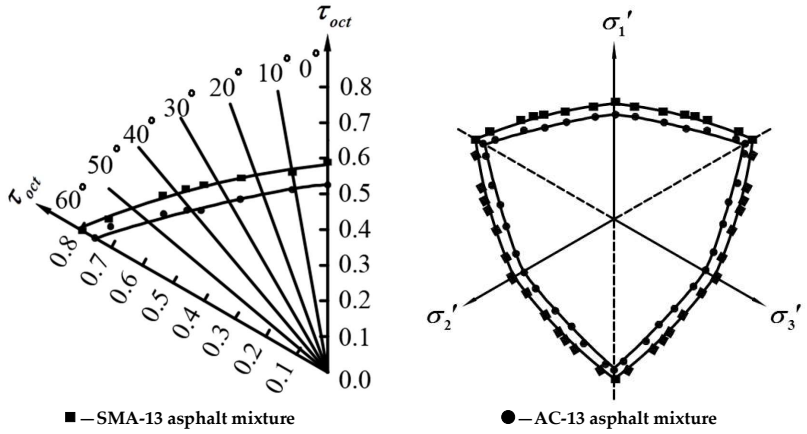

Figure 9. Nonlinear strength envelope curves in the π-plane.

It is shown that these failure criteria are in good agreement with the test results and reflect the difference between the tensile and compressive strength of the asphalt mixtures under complex stress states, as well as the synergistic failure effect of each stress component in the pavement structures.

However, these criteria are complicated and have many fitting parameters. In the process of regression, the tensile meridian can be approximated with a quadratic polynomial. The tensile and compressive meridians must intersect at the triaxial equal tensile point when $\tau_{oct} = 0$. The tensile meridian and compressive meridian were set at a proportion relationship to simplify the meridians. Furthermore, it is assumed that the strength envelope in the region of 0°~60° is interpolated with the sine function [29,30]. Therefore, the failure criteria can be represented as

Tensile meridian:

$$\frac{\tau_{oct}^{t}}{f_c} = a_1 + b_1\frac{\sigma_{oct}}{f_c} + c_1\left(\frac{\sigma_{oct}}{f_c}\right)^2,\ R_{AC}^2 = 0.94; R_{SMA}^2 = 0.99 \tag{7}$$

Compressive meridian:

$$\frac{\tau_{oct}^{c}}{f_c} = k\left[a_1 + b_1\frac{\sigma_{oct}}{f_c} + c_1\left(\frac{\sigma_{oct}}{f_c}\right)^2\right],\ R_{AC}^2 = 0.94; R_{SMA}^2 = 0.97 \tag{8}$$

Strength envelope curve:

$$\tau_{oct}(\theta) = \tau_{oct}^{t} - \left(\tau_{oct}^{t} - \tau_{oct}^{c}\right)\sin^m 1.5\theta,\ R_{AC}^2 = 0.94; R_{SMA}^2 = 0.97 \tag{9}$$

where a_1, b_1, c_1, k, and m are model parameters as shown in Table 5. The comparison with experiments is shown in Figures 8 and 9.

Table 5. Parameters of the simplified nonlinear failure criteria.

Mixture Type	a_1	b_1	c_1	k	m
AC-13	0.085	−0.67	−0.32	1.69	5
SMA-13	0.085	−0.664	−0.426	1.63	7

3.2. Linear Failure Criterion

As it is difficult for the engineering design department to establish the failure criteria, the nonlinear criteria should be further simplified for the convenience of analysis. Therefore, a linear failure criterion can be established by curve fitting as below [29].

Tensile meridian:

$$\frac{\tau_{oct}^t}{f_c} = a_2 + b_2\frac{\sigma_{oct}}{f_c},\ R_{AC}^2 = 0.94; R_{SMA}^2 = 0.96 \tag{10}$$

Compressive meridian:

$$\frac{\tau_{oct}^c}{f_c} = k_1\left(a_2 + b_2\frac{\sigma_{oct}}{f_c}\right),\ R_{AC}^2 = 0.94; R_{SMA}^2 = 0.98 \tag{11}$$

Strength envelope curve:

$$\tau_{oct}(\theta) = \tau_{oct}^t - (\tau_{oct}^t - \tau_{oct}^c)3\theta/\pi,\ R_{AC}^2 = 0.88; R_{SMA}^2 = 0.89 \tag{12}$$

where a_2, b_2, and k_1 are model parameters as shown in Table 6.

Table 6. Parameters of the linear failure criteria.

Mixture Type	a_2	b_2	k_1
AC-13	0.088	−0.733	1.4
SMA-13	0.08	−0.579	1.6

Seeing from Figures 9 and 10, the nonlinear failure envelope curves of asphalt mixtures are transformed from the shape similar to a shield into a hexagon in the $\sigma_{oct} - \tau_{oct}$ space due to linear fitting. With the increase of average stress, the hexagon strength envelope gradually expands along the linear tensile and compressive meridians as shown in Figure 11. Furthermore, the simplified failure criterion under complex stress states can be established by the uniaxial compressive, uniaxial tensile, and the ordinary triaxial tests. Although each of these tests cannot reflect the strength properties of asphalt mixtures under three-dimensional stress states, the synergistic failure effect of each stress component can be considered with the combination of these tests. Therefore, the engineering design department has the ability to complete the related tests.

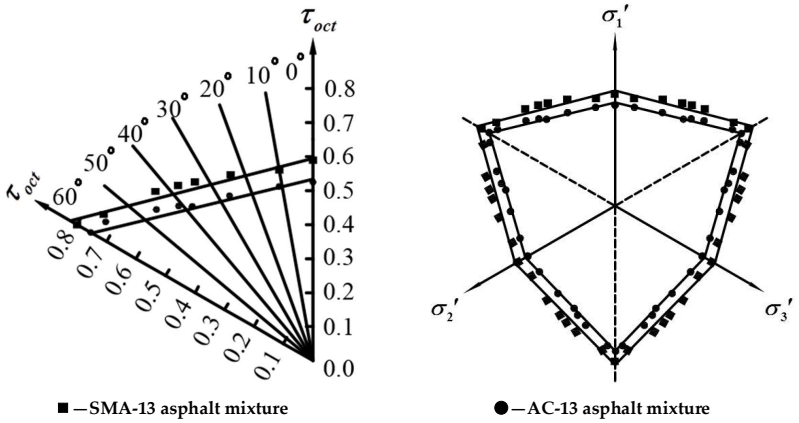

Figure 10. Linear strength envelope curves in the π-plane.

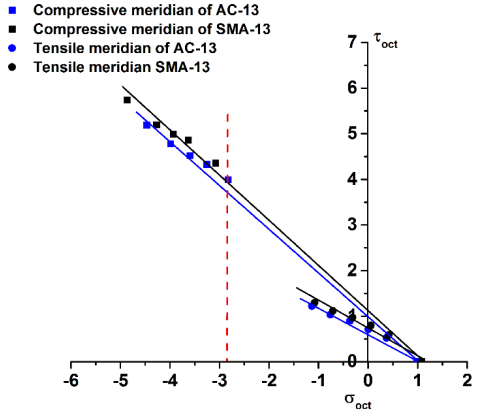

Figure 11. Linear tensile and compressive meridians.

3.3. Failure Criterion after Freeze-Thaw Cycles

According to the establishment of engineering failure criterion and its testing method, the failure criterion of AC-13 and SMA-13 asphalt mixtures following freeze-thaw cycles can be established by conducting uniaxial compressive, uniaxial tensile, and the conventional triaxial tests. The average value of three effective test results of failure strength after 0, 1, 3, 5, 10, 15, and 20 freeze-thaw cycles are listed in Table 7.

The three-dimensional failure criteria after freeze-thaw cycles can be represented by Tensile meridian:

$$\frac{\tau_{oct}^t}{f_c} = a_2 + b_2\frac{\sigma_{oct}}{f_c} - c_2 N,\ R_{AC}^2 = 0.85; R_{SMA}^2 = 0.83 \tag{13}$$

Compressive meridian:

$$\frac{\tau_{oct}^c}{f_c} = k_1\left(a_2 + b_2\frac{\sigma_{oct}}{f_c} - c_2 N\right),\ R_{AC}^2 = 0.98; R_{SMA}^2 = 0.98 \tag{14}$$

Strength envelope curve:

$$\tau_{oct}(\theta) = \tau_{oct}^t - (\tau_{oct}^t - \tau_{oct}^c)3\theta/\pi \tag{15}$$

where N is the number of freeze-thaw cycles; a_2, b_2 c_2, and k_1 are model parameters as shown in Table 8.

Table 7. Failure strength of asphalt mixtures after freeze-thaw cycles.

Mixture Type	Freeze-Thaw Cycles (*N*)	Uniaxial Compressive Strength	Triaxial Compressive Strength			Uniaxial Tensile Strength
		f_c (MPa)	σ_1 (MPa)	σ_2 (MPa)	σ_3 (MPa)	f_t (MPa)
AC-13	0	−8.477	−0.2	−0.2	−9.372	1.110
	1	−8.201	−0.2	−0.2	−9.194	1.072
	3	−7.913	−0.2	−0.2	−8.765	0.994
	5	−7.460	−0.2	−0.2	−8.451	0.936
	10	−6.866	−0.2	−0.2	−7.835	0.818
	15	−6.358	−0.2	−0.2	−7.423	0.733
	20	−6.104	−0.2	−0.2	−7.301	0.692
SMA-13	0	−9.240	−0.2	−0.2	−10.506	1.258
	1	−9.067	−0.2	−0.2	−10.287	1.217
	3	−8.634	−0.2	−0.2	−9.862	1.109
	5	−8.271	−0.2	−0.2	−9.643	1.043
	10	−7.596	−0.2	−0.2	−8.970	0.925
	15	−7.128	−0.2	−0.2	−8.553	0.844
	20	−6.714	−0.2	−0.2	−8.302	0.796

Table 8. Parameters of the linear failure criterions after freeze-thaw cycles.

Mixture Type	a_2	b_2	c_2	k_1
AC-13	0.088	−0.733	0.0015	1.4
SMA-13	0.08	−0.579	0.0012	1.6

The failure characteristics of AC-13 and SMA-13 asphalt mixtures after freeze-thaw cycles are similar to the previous failure modes. The specimens experienced shear failure and tensile failure and there are a few loose grains on the failure surfaces.

Seeing from Figures 12 and 13, there are multivariate linear relationships between the octahedral shear strength and the octahedral normal strength, as well as the freeze-thaw numbers of AC-13 and SMA-13 asphalt mixtures, the failure envelope curves also shrink during the freeze-thaw process. This criterion provides the testing and theoretical reference for material and structure design of asphalt pavement in three-dimensional stress states under freeze-thaw conditions.

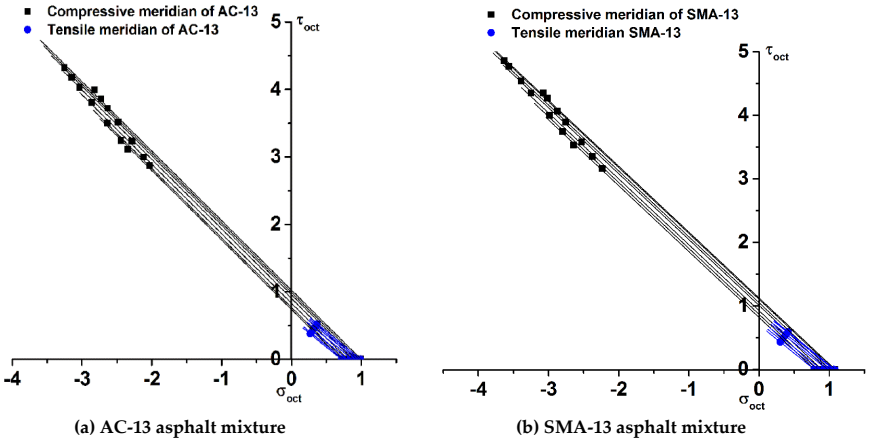

(a) AC-13 asphalt mixture (b) SMA-13 asphalt mixture

Figure 12. Tensile and compressive meridians of asphalt mixtures after freeze-thaw cycles. **Note:** The meridians from top to bottom represent the tensile and compressive meridians after 0, 1, 3, 5, 10, 15, and 20 freeze-thaw cycles, respectively.

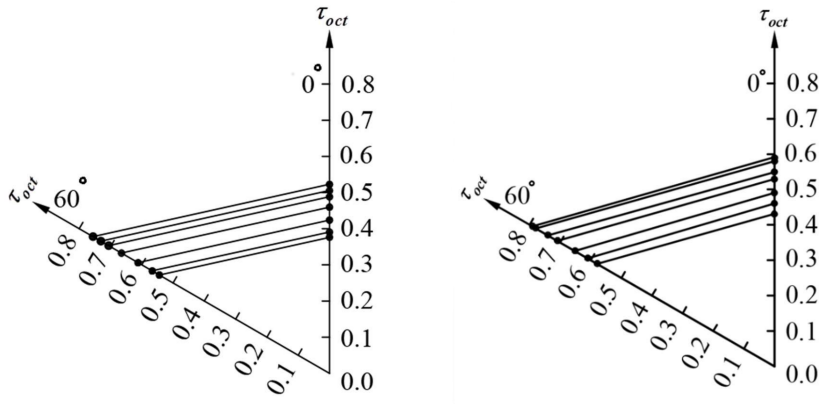

(a) AC-13 asphalt mixture (b) SMA-13 asphalt mixture.

Figure 13. Strength envelope curves of asphalt mixtures after freeze-thaw cycles. **Note:** The straight lines from outside to inside represent the failure envelope curves after 0, 1, 3, 5, 10, 15, and 20 freeze-thaw cycles, respectively.

As shown in Figure 14, the freeze-thaw process can degrade the resistance of three-dimensional stress states; the uniaxial compressive strength, triaxial compressive strength, and uniaxial tensile decayed significantly after 20 freeze-thaw cycles for these two asphalt mixtures. Especially, the strength degrades rapidly during the first 5 freeze-thaw cycles. Compared with the continuous-graded AC-13 asphalt mixture, the gap-graded SMA-13 asphalt mixture exhibits better resistance to freeze-thaw damage under complex stress conditions. This is mainly because SMA-13 is a framework-dense structure and AC-13 is a suspend-dense structure, the SMA-13 asphalt mixture consists of a coarse aggregate skeleton which has a high binder content and a low air void content, and there are some fibers in the mixture [31–33]. Since the influence of freeze-thaw cycling and complex stress conditions are inevitable in the middle and lower reaches of the Yangtze River and some seasonally frozen areas of China in winter, the SMA-13 asphalt mixture is recommended to improve the resistance to freeze-thaw erosion.

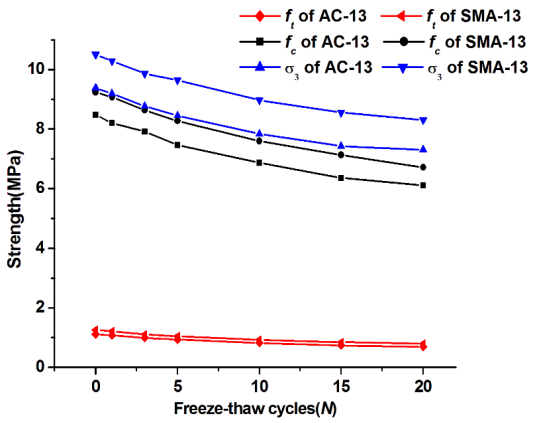

Figure 14. Strength of asphalt mixtures after freeze-thaw cycles.

4. Summary and Conclusions

Through the triaxial experiments, the nonlinear failure criterion with seven parameters and the simplified nonlinear failure criterion with five parameters have been established to characterize the mechanical behavior of AC-13 and SMA-13 asphalt mixtures under three-dimensional stress states. Furthermore, a linear engineering failure criterion with three parameters is also proposed. This criterion can be obtained by uniaxial compressive, uniaxial tensile, and conventional triaxial

compressive tests. With the linear criterion, the synergistic failure effect of each stress components can be considered which is also convenient for engineering analysis.

The three-dimensional failure criteria of AC-13 and SMA-13 asphalt mixtures after 0, 1, 3, 5, 10, 15, and 20 freeze-thaw cycles are presented based on the combination strength tests. There is a multivariate linear relationship between the octahedral shear strength, the octahedral normal strength, as well as the freeze-thaw numbers. Compared with the AC-13 asphalt mixture, the SMA-13 asphalt mixture exhibits better resistance to freeze-thaw damage under complex stress states. Therefore, the SMA-13 SBS asphalt mixture is recommended as the upper surface layer material of pavement structure.

Further analysis is required for asphalt mixtures with varying asphalt content or varying compaction in the lab to improve the three-dimensional resistance following freeze-thaw cycles. Meanwhile, data can be obtained by taking special samples from construction projects to conduct triaxial tests to establish actual failure criteria.

Author Contributions: Conceptualization (T.H. and S.L.); Data curation (T.H., S.Q., M.Y., S.L. and H.L.); Formal analysis (T.H. and S.L.); Funding acquisition (T.H., S.L. and J.Z.); Methodology (T.H. and H.L.); Project administration (T.H. and S.L.); Resources (T.H. and S.L.); Supervision (J.Z.); Writing—original draft (T.H., S.Q., M.Y. and S.L.); Writing—review & editing (T.H., S.Q., M.Y. and S.L.).

Funding: This research was funded by the National Natural Science Foundation of China [51608055, 51578081, 51608058], Construction Project of Science and Technology of Ministry of Transport of the People's Republic of China [2015318825120], Key Projects of Hunan Province-Technological Innovation Project in Industry [2016GK2096], Hunan Province Natural Science Foundation [2018JJ3550], Open Fund of the Key Laboratory of Highway Engineering of Ministry of Education (Changsha University of Science & Technology) [kfj160201].

Conflicts of Interest: The authors declare no conflict of interest.

References

1. Shang, H.; Song, Y.; Qin, L. Experimental study on strength and deformation of plain concrete under triaxial compression after freeze-thaw cycles. *Build. Environ.* **2008**, *43*, 1197–1204. [CrossRef]
2. Wang, D.; Chen, X.; Stanjek, H.; Oeser, M.; Steinauer, B. Influence of freeze-thaw on the polishing resistance of coarse aggregates on road surface. *Constr. Build. Mater.* **2014**, *64*, 192–200. [CrossRef]
3. Yu, X.; Liu, Y.; Gonzalez, J.; Yu, B. A new TDR sensor for accurate freeze-thaw measurement. *Int. J. Pavement Eng.* **2012**, *13*, 523–534. [CrossRef]
4. Wang, Y.; Ye, J.; Liu, Y.; Qiang, X.; Feng, L. Influence of freeze-thaw cycles on properties of asphalt-modified epoxy repair materials. *Constr. Build. Mater.* **2013**, *41*, 580–585. [CrossRef]
5. Tang, N.; Sun, C.; Huang, S.; Wu, S. Damage and corrosion of conductive asphalt concrete subjected to freeze-thaw cycles and salt. *Mater. Res. Innov.* **2013**, *17*, 240–245. [CrossRef]
6. Yan, K.; You, L.; Wang, X. Test on characteristics of SMA mixtures under freeze-thaw cycle and ultrasonic evaluation method. *China J. Highw. Transp.* **2015**, *11*, 8–14.
7. El-Hakim, M.; Tighe, S. Impact of freeze-thaw cycles on mechanical properties of asphalt mixes. *Transp. Res. Rec. J. Transp. Res. Board* **2014**, *2444*, 20–27. [CrossRef]
8. Kettil, P.; Engström, G.; Wiberg, N.E. Coupled hydro-mechanical wave propagation in road structures. *Comput. Struct.* **2015**, *83*, 1719–1729. [CrossRef]
9. Feng, D.; Yi, J.; Wang, D.; Chen, L. Impact of salt and freeze-thaw cycles on performance of asphalt mixtures in coastal frozen region of China. *Cold Reg. Sci. Technol.* **2010**, *62*, 34–41. [CrossRef]
10. Lv, S.; Liu, C.; Yao, H.; Zheng, J. Comparisons of synchronous measurement methods on various moduli of asphalt mixtures. *Constr. Build. Mater.* **2018**, *158*, 1035–1045. [CrossRef]
11. Kakade, V.B.; Reddy, M.A.; Reddy, K.S. Evaluation of the sensitivity of different indices to the moisture resistance of bituminous mixes modified by hydrated lime and other modifiers. *Road Mater. Pavement Des.* **2017**, *18*, 1395–1410. [CrossRef]
12. You, L.; Yan, K.; Hu, Y.; Ma, W. Impact of interlayer on the anisotropic multi-layered medium overlaying viscoelastic layer under axisymmetric loading. *Appl. Math. Model.* **2018**, *61*, 726–743. [CrossRef]
13. Lv, S.; Zheng, J. Normalization method for asphalt mixture fatigue equation under different loading frequencies. *J. Cent. South Univ.* **2015**, *22*, 2761–2767. [CrossRef]

14. Lv, S.; Wang, S.; Liu, C.; Zheng, J.; Li, Y.; Peng, X. Synchronous Testing Method for Tension and Compression Moduli of Asphalt Mixture under Dynamic and Static Loading States. *J. Mater. Civ. Eng.* **2018**, *30*, 04018268. [CrossRef]
15. Lv, S.; Wang, X.; Liu, C.; Wang, S. Fatigue Damage Characteristics Considering the Difference of Tensile-Compression Modulus for Asphalt Mixture. *J. Test. Eval.* **2018**, *46*, 20170114. [CrossRef]
16. Xu, H.; Guo, W.; Tan, Y. Internal structure evolution of asphalt mixtures during freeze thaw cycles. *Mater. Des.* **2015**, *86*, 436–446. [CrossRef]
17. Shakiba, M.; Darabi, M.K.; Al-Rub, R.K.A.; You, T.; Little, D.N.; Masad, E.A. Three-dimensional microstructural modelling of coupled moisture-mechanical response of asphalt concrete. *Int. J. Pavement Eng.* **2015**, *16*, 445–466. [CrossRef]
18. Tan, Y.; Zhao, L.; Lan, B.; Liang, M. Research on freeze-thaw damage model and life prediction of asphalt mixture. *J. Highw. Transp. Res. Dev.* **2011**, *28*, 1–7.
19. Yi, J.; Shen, S.; Muhunthan, B.; Feng, D. Viscoelastic–plastic damage model for porous asphalt mixtures: Application to uniaxial compression and freeze-thaw damage. *Mech. Mater.* **2014**, *70*, 67–75. [CrossRef]
20. You, L.; Yan, K.; Hu, Y.; Liu, J.; Ge, D. Spectral element method for dynamic response of transversely isotropic asphalt pavement under impact load. *Road Mater. Pavement Des.* **2018**, *19*, 223–238. [CrossRef]
21. Lv, S.; Liu, C.; Chen, D.; Zheng, J.; You, Z.; You, L. Normalization of fatigue characteristics for asphalt mixtures under different stress states. *Constr. Build. Mater.* **2018**, *177*, 33–42. [CrossRef]
22. Su, Y.M.; Hossiney, N.; Tia, M. Indirect tensile strength of concrete containing reclaimed asphalt pavement using the superpave indirect tensile test. *Adv. Mater. Res.* **2013**, *723*, 368–375. [CrossRef]
23. Park, S.W.; Kim, Y.R.; Schapery, R.A. A viscoelastic continuum damage model and its application to uniaxial behavior of asphalt concrete. *Mech. Mater.* **1996**, *24*, 241–255. [CrossRef]
24. Kutay, M.E.; Aydilek, A.H. Dynamic Effects on Moisture Transport in Asphalt Concrete. *J. Transp. Eng.* **2007**, *133*, 406–414. [CrossRef]
25. Tan, S.A.; Low, B.H.; Fwa, T.F. Behavior of asphalt concrete mixtures in triaxial compression. *J. Test. Eval.* **1994**, *22*, 195–203. [CrossRef]
26. Hofko, B.; Blab, R. Enhancing triaxial cyclic compression testing of hot mix asphalt by introducing cyclic confining pressure. *Road Mater. Pavement Des.* **2014**, *15*, 16–34. [CrossRef]
27. Huang, T.B. *Study on Strength Properties of Asphalt Mixture under Complex stress state*; Central South University Press: Changsha, China, 2013.
28. Zheng, J.; Huang, T. Study on triaxial test method and failure criterion of asphalt mixture. *J. Traffic Transp. Eng.* **2015**, *2*, 93–106. [CrossRef]
29. Huang, T.; Zheng, J.; Lv, S.; Zhang, J.; Wen, P.; Bailey, C.G. Failure criterion of an asphalt mixture under three-dimensional stress state. *Constr. Build. Mater.* **2018**, *170*, 708–715. [CrossRef]
30. Song, Y. *Constitutive Relations and Failure Criterions of Various Concrete Materials*; China Water Conservancy and Hydropower Press: Beijing, China, 2002.
31. Cao, X.; Tang, B.; Zhu, H.; Chen, S. Cooling principle analyses and performance evaluation of heat-reflective coating for asphalt pavement. *J. Mater. Civ. Eng.* **2011**, *23*, 1067–1075. [CrossRef]
32. Tarefder, R.; Faisal, H.; Barlas, G. Freeze-thaw effects on fatigue LIFE of hot mix asphalt and creep stiffness of asphalt binder. *Cold Reg. Sci. Technol.* **2018**, *153*, 197–204. [CrossRef]
33. Özgan, E.; Serin, S. Investigation of certain engineering characteristics of asphalt concrete exposed to freeze-thaw cycles. *Cold Reg. Sci. Technol.* **2013**, *85*, 131–136. [CrossRef]